HERPESVIRUS-MEDIATED DELIVERY OF A GENETICALLY ENCODED FLUORESCENT CA^{2+} SENSOR TO CANINE CARDIOMYOCYTES

János Prorok[a], Péter P. Kovács[a], Attila A. Kristóf[c], Norbert Nagy[a], Dóra Tombácz[b], Judit S. Tóth[b], Balázs Ördög[b], Norbert Jost[c], László Virág[a], Julius G. Papp[a,c], András Varró[a], András Tóth[a#], Zsolt Boldogkői[b#]

[a]Department of Pharmacology & Pharmacotherapy, [b]Department of Medical Biology, Faculty of Medicine, University of Szeged, [c]Division of Cardiovascular Pharmacology, Hungarian Academy of Sciences, Szeged, Hungary

Running head: Gene transfer to adult myocytes by a herpes virus vector

[#] Drs A. Tóth and Z. Boldogkői share senior authorship

To whom correspondence should be addressed:

Zsolt Boldogkői

Department of Medical Biology

Faculty of Medicine, University of Szeged

H-6720 Szeged, Somogyi B. u. 4.

Hungary

Tel: (36) (62) 545-595

Fax: (36) (62) 545-131

E-mail: boldog@sb4.szote.u-szeged.hu

Abstract

In this study, we report the development and application of a pseudorabies virus-based system for delivery of troponeon, a fluorescent Ca^{2+} sensor to adult canine cardiomyocytes. The efficacy of transduction was assessed by calculating the ratio of fluorescently labelled and non-labelled cells in cell culture. Interaction of the virus vector with electrophysiological properties of cardiomyocytes was evaluated by the analysis of transient outward current (I_{to}), kinetics of the intracellular Ca^{2+} transients and cell shortening. Functionality of transferred troponeon was verified by FRET analysis. We demonstrated that the transfer efficiency of troponeon to cultured adult cardiac myocytes was virtually 100%. We showed that even after four days neither the amplitude nor the kinetics of the I_{to} current was significantly changed and no major shifts occurred in parameters of $[Ca^{2+}]_i$ transients. Furthermore, we demonstrated that infection of cardiomyocytes with the virus did not affect the morphology, viability and physiological attributes of cells.

Keywords: pseudorabies virus, herpes virus, gene transfer, troponeon, cardiomyocytes, cell culture, I_{to}, calcium transient, FRET

1. Introduction

The past decade has witnessed an explosive progress of virus-based gene delivery technologies. The reason for this is that, albeit traditional approaches, such as calcium phosphate precipitation, electroporation, or liposome-mediated gene transfer perform excellently in immortalized cells of various origins, they mostly fail in primary cultured cells and under *in vivo* conditions. Viruses had millions of years to evolve several means for effective infection of cells that can be employed by utilizing viruses as vectors for delivering exogenous genes to the desired cells. Virus-mediated gene transfer methods have also become powerful and widely used experimental tools in cardiovascular research. The most important prerequisites for successful *in vitro* gene transfer into adult cardiomyocytes include high quality of primary cell culture and an effective transfer vector with limited cytotoxicity and other side effects. However, adult cardiomyocytes are difficult to transduce using methods that work well in other systems because cardiac cells do not divide, have a relatively short lifetime in culture and are highly sensitive to toxic effects. Gene transfer methods used in cardiovascular research can be divided into two groups: physicochemical and viral vector-based systems. Non-viral methods involve cationic liposome/plasmid DNA complexes, incubation with naked DNA, and calcium phosphate precipitation [1, 2]. All of these methods suffer from severe limitations such as cytotoxicity, very low transfection efficiency especially *in vivo* applications, and short-term expression of transduced genes due to intracellular degradation of foreign DNA. The above limitations urged the application of more efficient virus vector-based approaches for gene delivery to the cardiovascular system. The following viral systems have been applied in molecular cardiology: adenovirus vectors (Ads), adeno-associated viruses (AAVs), retroviruses (RV) like lentivirus (HIV-1) and herpes simplex virus (HSV-1)-derived vectors [1, 2]. Currently, Ads and AAVs

are the most frequently used tools for delivering genes into the cells of the cardiovascular system, both *in vivo* and *in vitro* [3, 4]. While Ads–based vectors allow relatively highly efficient delivery of transgenes to cardiac cells, this system provides only transient expression of transferred genes since the virus does not integrate into the host genome [5]. The application of Ads have further limitations including strong immune responses by the host organism, limited space for transgene integration and during adaptation may have moderately difficult quality control. An additional problem with Ads systems is related to the infection efficiency. The coxsackie adenovirus receptor (CAR) is a key determinant for the attachment and cellular uptake of adenoviruses [6]. However, CAR expression is maximal in neonates and gets reduced rapidly after birth in several organs such as heart, muscle and brain resulting in lower penetration rate of adenovirus vectors [7].

Recombinant AAV vectors are able to effectively transduce foreign genes to a variety of cell types including both dividing and post-mitotic cells in both *in vitro* and *in vivo* experimental systems [8]. The AAV-based systems have a number of favourable attributes, such as lack of parental agent pathogenicity and vector-related cytotoxicity, minimal immunogenicity, and the capacity for stable long-term transgene expression. The main disadvantages of AVV vector–based approaches include the difficulty of producing high-titer virus stocks of consistent purity and bioactivity, and the limited packaging capacity of a maximum 4.8 kb insert-size [9]. Lentivirus-based gene transfer has been reported in a wide variety of cell types, including cardiomyocytes [10]. Current lentiviral vectors are capable of transducing mitotically quiescent cells, particularly within the cardiovascular system. The strengths of this system include the ability of long-term stable transgene expression, an increased packaging capacity compared with AAV, and the other commonly used integrating vector [11]. The

disadvantages of lentivirus-based gene delivery systems are the relative low level of transgene expression and the limited transgene carrying capacity of the virus.

Pseudorabies virus (PRV), a causative agent of Aujeszky's disease of swine, is an alpha-herpesvirus belonging to family of Herpesviridae. Several previous reports have been successful in construction of PRVs for delivering foreign genes to neurons [12]. PRV is especially an important tool for labelling neural circuits [13], which was combined with delivery of activity markers to labelled neurons [14].

In this study, we have developed a method for short-term culture of isolated myocytes that retains their morphological as well as physiological integrity and a pseudorabies virus (PRV)-based system for delivery of foreign genes to adult cardiac muscle cells. Troponeon (TN-L15) [15], a FRET-based activity marker was selected as a model transgene system. Troponeon is a genetically-encoded fluorescent Ca^{2+} sensor that is suitable for the imaging of cellular activity in neurons, muscle and cardiac cells. Pseudorabies virus was modified to disable to replicate on post-mitotic cells but retaining its capacity for high titer multiplication on dividing cultured epithelial cells. The strengths of the presented system is a very high gene transfer efficiency, low toxic effect, the capacity for relative long-term transgene expression, and the delivery of large or multiple transgenes. The suitability of PRV-based gene delivery technique was evaluated in several ways. We performed simultaneous measurements in non-infected control and infected myocytes following isolation and infection. Retained functionality of the sarcolemmal ion channels was tested by measuring a characteristic multichannel current I_{to}. Intactness of the excitation contraction coupling (ECC) machinery and contractile function was demonstrated by monitoring intracellular calcium transients and cell shortening. Finally, undisturbed functioning of the transmitted gene was verified by FRET monitoring of the calcium transient currents.

2. Materials and Methods

2.1 Cells and viruses

The wild type Kaplan strain [16] of pseudorabies virus (PRV) was used as parent strain for the generation of recombinant viruses used in this study. Viruses were propagated on subconfluent monolayer of porcine kidney (PK-15) cells. Cells were grown in DMEM supplemented with 5% fetal calf serum at 37°C with 5% CO2. The stocks of PRV were prepared as follows: PK-15 cells were infected with PRV at a multiplicity of 1 p.f.u/cell, harvested after 24h, followed by freezing and thawing three times. The cells were then centrifuged and the pellet discarded. The supernatant fluid was stored in 400 μl aliquots at -80°C.

2.2 Reporter genes

Tn-15 (troponeon), a FRET-based fluorescent calcium sensor [15], was used as an activity marker in our experiments. The troponeon gene was placed under the control of the major immediate early promoter of human cytomegalovirus (pCMV), which provided a high level of gene expression. The marker gene expression cassette also contained simian virus 40 (SV40)-derived sequences including polyadenylation signal and transcription termination sequences. In addition, a lacZ gene equipped with the above regulatory sequences was also used as a reporter gene for the identification of mutant viruses.

2.3 Construction of targeting vectors

In our system, a typical targeting plasmid contains a marker gene expression cassette flanked by subcloned viral DNA sequences, which serves as homologous DNA regions

for the insertion of marker genes via homologous recombination. The DNA sequences used for mutagenesis and as insertion sites for reporter genes are listed on Figure 1.

Ribonucleotide reductase (RR) gene The details of the construction of RR gene targeting vector was described elsewhere [17]. Briefly, a 5-kbp *Sal*I-F fragment of PRV DNA containing both subunits of RR gene was isolated and cloned to pRL494, a palindrome-containing positive selection vector [18]. This plasmid was cut with *Sca*I and *Mlu*I restriction endonucleases generating a 1,805-bp deletion, which included a 1,789-bp DNA fragment from the 3' end of large (RR1) and a 7-bp DNA sequence from the 5' end of small subunit (RR2) of ribonucleotide reductase gene. Subsequently, free DNA ends were filled up by Klenow enzyme followed by attaching an *Eco*RI linker to the blunt DNA ends. As a final step, a lacZ gene expression cassette bracketed by *Eco*RI sites was subcloned to the *Eco*RI site of this plasmid.

Early protein 0 (EP0) gene Generation of EP0 gene targeting vector was described previously [19]. Briefly, the 9.4-kb *Kpn*I-F DNA fragment containing the EP0 gene was subcloned into pRL425; followed by cleaving with *Bam*HI restriction endonuclease, which resulted in the deletion of a 1390-bp sequence, including almost the entire EP0 gene. Free DNA ends were converted to *Eco*RI sites via linker insertion and then religated. The same lacZ gene expression cassette as above was subcloned to the *Eco*RI site of this plasmid.

Putative antisense promoter (ASP) region The 4.9-kb *Bam*HI-8' PRV DNA fragment was isolated and subcloned to pRL525 cloning vector [18, 20]. The *Dra*I site located in the putative TATAA box of ASP was used for the insertion of *Eco*RI thereby destroying its potential function. The fluorescent marker gene expression cassettes (GFP, troponeon) were inserted to the *Eco*RI site of this plasmid.

2.4 Generation and isolation of recombinant viruses

Recombinant viruses were generated by means of homologous recombination between parent PRV genomes and targeting plasmids containing reporter genes bracketed by virus sequences. Viral DNA was transfected to actively growing PK-15 cells along with the appropriate targeting plasmid using lipid-mediated gene delivery (Lipofectamine 2000 Reagent, Invitrogen). Viral DNA for the transfection was prepared from virions purified from the medium of infected cells showing total cytopathic effects by isopycnic centrifugation on a discontinuous gradient, as described previously [12]. The *lacZ* gene-expressing viruses were screened based on their blue plaque appearance in the presence of 5-bromo-4-chloro-3-indolyl-*b*-D-galactopyranoside (X-Gal), the chromogenic substrate of *β*-galactosidase. Blue plaques were picked and plaque purified to complete homogeneity. Plaques formed by recombinant viruses carrying the fluorescent markers were detected visually on the basis of their fluorescence. Recombinant viruses were isolated by 6-15 cycles of plaque purification procedure using a fluorescence microscope (Olympus IX-71).

2.5 Isolation of adult canine cardiomyocytes

All experiments were conducted in compliance with the *Guide for the Care and Use of Laboratory Animals* (USA NIH publication No 85-23, revised 1985). The protocols were approved by the review board of the Committee on Animal Research (CAR) of the Albert Szent-Györgyi Medical University. The modified protocol for cell isolation was based on established procedures described earlier in detail [21].

Canine ventricular myocytes were enzymatically dissociated as follows. A portion of the left ventricular wall containing an arterial branch large enough to cannulate was perfused in a modified Langendorff apparatus with solutions in the following sequence: 1) normal Tyrode's solution (10 min), 2) Ca^{2+}-free Tyrode solution (10 min), and 3)

Ca^{2+}-free Tyrode solution containing collagenase (type I, 0.66 mg/ml) and bovine serum albumin (fraction V, fatty acid free, 2 mg/ml) (15 min). Protease (type XIV, 0.12 mg/ml) was added to the final perfusate while and another 15 - 30 min of digestion was allowed. Cells were stored in KB solution. The composition of solutions were (in mM): *a) normal Tyrode's solution* - NaCl 135, KCl 4.7, KH_2PO_4 1.2, $MgSO_4$ 1.2, HEPES 10, $NaHCO_3$ 4.4, glucose 10, and $CaCl_2$ 1.0 (pH 7.2 adjusted with NaOH); *b)* Ca^{2+}*-free Tyrode solution* - NaCl 135, KCl 4.7, KH_2PO_4 1.2, $MgSO_4$ 1.2, HEPES 10, $NaHCO_3$ 4.4, Glucose 10, and taurine 20 (pH 7.2 adjusted with NaOH); c) *KB solution* - KOH 90, L-glutamic acid 70, taurine 15, KCl 30, KH_2PO_4 10, $MgCl_2$ 0.5, HEPES 10, glucose 11, and EGTA 0.5 (pH 7.3 adjusted with KOH). All chemicals used in this method were purchased from Sigma Chemical Co.

2.6 Culture and infection of myocytes

The entire culture procedure was performed in a class II flow hood. The freshly isolated myocytes were centrifuged five times for 1 min at 50 g in sterile 10% PBS. The supernatant was replaced first by 500 μM then by 1 mM Ca^{2+} containing PBS solution. The mild centrifugation steps removed the majority of bacterial cells, most non-myocytes and non-functioning myocytes. Precipitated cells were resuspended in culture medium and plated on laminin coated (1 $\mu g/cm^2$) sterile cover glass at densities of up to 10^3 rod-shaped cells cm^{-2}. Cells were left 4 hours to attach to the plate and after this time period non attached cells were removed. Following the first medium change, subsequent medium changes were carried out every day. Culture medium consisted of serum-free medium 199 (M199) supplemented with 25 mM $NaHCO_3$, 5 mM ceratine, 2 mM L-carnitine, 5 mM taurine, 100 units/ml insulin (CCTI supplemented medium) and 50μg/ml gentamycin. All chemicals used in this procedure were purchased from Sigma. Cells were maintained at 37°C under sterile conditions in an incubator ventilated with

5% CO_2 and 95% air. After 4 hours, plate attached cells were infected. Freshly isolated canine cardiomyocytes were first washed with PBS, followed by low-speed centrifugation and resuspension in culture medium. Subsequently, after a 4-hour incubation at 37C° in a CO_2 incubator, cells were infected with various titers of recombinant viruses for 12 hours then washed and the culture medium was changed. Infected cells were used for analysis at various time points.

2.7 Evaluation of infection efficacy and morphological changes in cultured cardiomyocytes

Cell shape and morphology are closely linked with some aspects of cell function such as excitation–contraction coupling. Therefore, monitoring these properties may give indications of physiological changes that are occurring. Morphological changes of cells were observed by light microscope on a daily basis parallel with physiological measurements. Troponeon-positive cells were examined by fluorescence microscopy from one to three days following isolation at standard titer of viruses. Infection efficacy was determined separately for infected cells by manual cell counting using a fluorescent microscope (Olympus IX-71).

2.8 Evaluation of the physiological state of the virus infected cells

2.8.1. Evaluation of the electrophysiological state of the cells by I_{to} analysis

I_{to} currents were measured at 37 ºC using the whole-cell configuration of the patch-clamp technique. Measurements were performed daily starting with day 0, when only freshly isolated non-infected myocytes were investigated. In the following days control and infected cells were studied separately by placing cover glasses with the attached cells in the recording chamber mounted on the stage of an inverted microscope equipped with epifluorescence assembly (Olympus IX50, Tokyo, Japan). Only rod-

shaped cells with clear cross striations and relatively strong GFP signal were used. HEPES-buffered Tyrode's solution containing (in mM): NaCl 144, NaH_2PO_4 0.33, KCl 4.0, $CaCl_2$ 1.8, $MgCl_2$ 0.53, glucose 5.5 and HEPES 5.0 at pH of 7.4 (by NaOH) served as normal superfusate. Cell capacitance (199.3±13.7 pF, n=69) was determined by applying a 10 mV hyperpolarizing pulse from a holding potential of -10 mV. Cell capacity was calculated as the integral of the capacitive transient divided by the amplitude of the voltage step. Patch-clamp micropipettes were fabricated from borosilicate glass capillaries (Clark, Reading, UK) using a P-97 Flaming/Brown micropipette puller (Sutter Co, Novato, CA, USA). These electrodes had resistances between 1.5 and 2.5 Mohms when filled with pipette solution containing (in mM): K-aspartate 100, KCl 45, K_2ATP 3, $MgCl_2$ 1, EGTA 10 and HEPES 5. The pH of this solution was adjusted to 7.2 by KOH. Nisoldipine (1 μM) (obtained as a gift from the Bayer AG, Leverkusen, Germany) was used in the external solution to eliminate inward Ca^{2+} current (I_{Ca}). Membrane currents were recorded with Axopatch-200B patch-clamp amplifiers (Axon Instruments, Foster City, CA, USA). After establishing a high (1-10 Gohm) resistance seal by gentle suction, the cell membrane beneath the tip of the electrode was disrupted by suction or by application of 1.5 V electrical pulses for 1 - 5 ms. The series resistance was typically 4 - 8 Mohm before compensation (50 - 80%, depending on the voltage protocols). Experiments where the series resistance was high, or substantially increased during measurement, were discarded. Membrane currents were digitized using a 333 kHz analogue-to-digital converter (Digidata 1200, Axon Instruments) under software control (pClamp 8.0, Axon Instruments). Analyses were performed using pClamp 8.0 (Axon Instruments) software after low-pass filtering at 1 kHz. All patch-clamp data were collected at 37 °C.

2.8.2. Evaluation of cell function by monitoring $[Ca^{2+}]_i$ transient and cell shortening

24-72 hours following viral infection cultured myocytes were loaded by incubation for 20 min with the acetoxymethyl ester (AM) form of a single wavelength calcium-sensitive fluorescent dye (Fluo-4, Molecular Probes Inc. 1–2μM from a stock of 1mM in DMSO + 20% pluronic acid) at room temperature. The technique for calcium transient detection was based on established procedures described earlier [22]. After this incubation period the cover glass with attached cultured myocytes was mounted in a low volume imaging chamber (RC47FSLP, Warner Instruments, USA) and placed on the stage of an inverted fluorescent microscope (IX71, Olympus, Japan). The cells were superfused with normal Tyrode solution at 37ºC (1ml/min). Myocytes were stimulated at a constant frequency of 1 Hz through a pair of platinum electrodes by an electronic stimulator. The dye was excited at 480 nm, fluorescence emission was recorded at 535 nm (Chroma, USA). Optical signals were recorded by a photon counting photomultiplier module (H7828, Hamamatsu, Japan), and sampled at 1 kHz. Measurements were performed and data were analyzed using the Isosys software (Experimetria Ltd, Hungary). Cell shortening from both ends was determined by a video edge detection system (VED-105, Crescent Electronics, Sandy, Utah, USA). All experiments were performed at 37 °C, using an automatic temperature controller (TC-344B, Warner Instruments, USA).

2.8.3. Evaluation of the functionality of the transferred gene by FRET measurement

For testing the functionality of the transferred gene, following the incubation period the cover glass with the attached primary cultured cardiomyocytes was mounted in a low volume imaging chamber (RC47FSLP, Warner Instruments, USA) on the stage of an

Olympus IX71 inverted microscope outfitted with a 75 W Xe arc lamp for epi- and a 100 W tungsten-halogen lamp for transillumination.. The myocytes in the chamber were superfused with normal Tyrode solution (1ml/min) and stimulated at a constant frequency of 1 Hz by an electronic stimulator (Experimetria) through a pair of platinum electrodes. All measurements were performed at 37 °C, by using an automatic temperature controller (TC-344B, Warner Instruments, USA). The optical signals were typically monitored 20-36h after infection in selected myocytes expressing the genetically encoded FRET-based sensor troponeon (csTnC-L15). Cells with medium-high level of fluorescence were selected for measurement. Though often troponeon fluorescence is already visible 16h following infection, optical signals were found to be optimal for recording after 24h.

Fluorescent optical signals were monitored by a dual channel photon counting system. An Olympus filter cube containing a CFP excitation filter (436/20x) and a CFP dichroic mirror (455DCLP) but no emission filter, was inserted into the light path of the microscope. A connector box for dual emission fluorescence with two interchangeable dichroic mirror holders and three detector ports (P226/0II/011, Cairn Research Ltd, UK) equipped with two photon counting photomultiplier modules (H7828, Hamamatsu, Japan) was attached to the left side port of the microscope. The fluorescent signal from the microscope was splitted by a YFP dichroic mirror (515LP). A second dichroic mirror (565DCLP) was used to separate the longer wavelength (FRET) fluorescence from the red filtered (> 580 nm) transillumination light used for visual observation of the cell by a video camera mounted on the 3rd, back port of the connector box. The splitted fluorescence components were band pass filtered (480/30m and 535/30m for CFP and citrine, respectively), integrated with 1 ms time resolution by two photon to voltage converter units (Ionoptics, US) and collected for data processing.

All interference filters and dichroic mirrors used are avaiable in filter sets 31036V2 and 41028 from Chroma Technology Corporation (US).

Changes in $[Ca^{2+}]_i$ levels were characterized by the ratio of the emitted fluorescence intensities obtained at 480 and 535 nm wavelengths, ($F_{FRET\_CITRINE}$ 535/ F_{CFP} 480) following optical signal correction steps for photobleaching and non-specific background fluorescence. Photobleaching leads to a steady decrease in the FRET ratio over time, because citrine is less photostable than CFP. To correct for bleaching, we multiplied the intensity of the CITRINE channel by a correction factor calculated from the intensity shift between two time points. For background correction we subtracted from the optical signals the nonspecific background fluorescence determined at both wavelengths by moving off the cell from the light path: $F_{RATIO\_corr} = (F–F_0)_{CITRINE} / (F–F_0)_{CFP}$. The background-corrected fluorescence ratio versus time curve can be considered as a representation of the intracellular Ca^{2+} transients (Fig 7).

2.9 Data analysis

All patch-clamp results and optical measurements were compared using Student's t-tests for paired and unpaired data and expressed as mean ± SEM values. Statistical significance of differences obtained between control and virus infected preparations was evaluated with Student’s t-test for paired or unpaired data, as relevant. Differences were considered significant when $p<0.05$.

3. Results

3.1 Morphological changes of cultured cardiomyocytes

Using the described method for isolation of adult dog left ventricular myocytes, we routinely obtained a high yield (more than 80%) and high (more than 80%) percentage of rod-shaped myocytes that were suitable not only for acute functional studies but, more importantly, for short-term culture and gene transfer. Figure 2A shows a trans-illumination image of freshly isolated and 1-day-old cultured cardiomyocytes from the left ventricle. To establish optimal surviving conditions several culture conditions were tested based on microscopic evaluation of changes in cellular morphology during the four days of culture. Cultured cells were used 1-3 days after isolation. During this period, visible small-scale changes in cell shape and cross-striation could be observed. Figure 2B shows representative photographs of canine myocytes over time in culture. Features typical of acutely isolated (Day 0) cells were the rod shape with rectangular stepped ends and clear cross-striations. After 1 day (Day 1) in culture, the cells were still rod-shaped with clear cross-striations; however, the ends of the cells started to become slightly rounded in appearance. After 3 days (Day 3) in culture, cells remained rod-shaped and cross-striated, and the main change was that cell ends became progressively more rounded (see Table 1 for cell survivals).

3.2 Efficacy of virus infection in cultured cardiomyocytes

Survival rates were found to be dependent on the isolation procedure, density of the attached myocytes and the applied virus titer. Intriguingly, a higher total number of viable cells were observed on the laminin-coated surfaces after plating in CCTI supplemented medium. As respective panels of Fig 2 and 3 (upper panel) show, even after three days, the cell culture contained a substantial number of good quality cells

both in the control and virus infected groups. Surprisingly, a moderately but consistently higher cell survival rate was found in virus infected groups as compared to non-infected groups (not shown). The infection efficiency was found to be 100%, that is 24h post-infection every surviving cells emitted fluorescent signals provided that high dose of virus was used for the infection (Fig 3 bottom panel).

3.3 Whole-cell patch-clamp recordings

The whole-cell configuration of the patch-clamp technique was used to record the transient outward I_{to} current. I_{to} was chosen as a physiological assay because it is a large current that can be measured relatively easily in isolated canine ventricular myocytes. The current was activated by 300 ms long depolarizing voltage pulses from the holding potential of -90 mV to test potentials ranging from 0 to +60 mV with a pulse frequency of 0.33 Hz. The amplitude of I_{to} was measured as the difference between the peak and the sustained current at the end of the voltage pulse. Figures 4A shows typical recordings of I_{to} measured after one (Day 1) and three days (Day 3) of culture either in control (top panels) or virus infected cells (bottom). Figure 4B summarizes all I_{to} measurements performed after 0-4 days of culture in both groups. As the corresponding panels of Figure 4 show, the amplitude of the I_{to} was reduced by less than 10% in virus infected myocytes (VM) compared to control non-infected cells (CM) even after 4 elapsed days. Moreover current amplitude was somewhat larger in PRV-infected cells compared to that of observed in control cells. Mean I_{to} density (Fig. 4B) was similar for CM and VM cells after 1 day. The I_{to} current density in VM changed in four days from 19.6 ±1.4 to 24.6±2.6 pA/pF (n=10-12), which corresponds well with that observed in CM (from 19.3±2.1 to 17.1±1.5 pA/pF, n=8-10). Although mean I_{to} density of several-day-old (2, 3, 4) cultured myocytes was significantly larger in VM than CM. The I_{to}

kinetics (activation and inactivation properties) was also not significantly altered by the virus infection.

3.4 Parameters of intracellular Ca^{2+} transients and contractility

Cultured myocytes were stimulated at a constant frequency of 1 Hz through a pair of platinum electrodes. Similarly to I_{to} measurements, the steady-state $[Ca^{2+}]_i$ transient and contractile function were measured and compared on a daily basis both in the infected and control cell populations. Original recordings of $[Ca^{2+}]_i$ transients and cell shortening before and after virus infection are presented in Figure 5. The calcium transient kinetics were significantly distorted in culture, but were also not significantly altered by the virus infection. As Figure 6 summarizes, we found no statistically significant differences in either the amplitude of calcium transient (A) or diastolic calcium level (B) between the studied groups. Moreover, transient decay time (C) in non-infected control myocytes was significantly larger than in the virus infected group after two and three days in culture. Conversely in virus-infected group's decay time was similar to freshly isolated cells. These results suggest that the normal control cell population may be lost their some calcium removal mechanism. The cell-shortening measurements (D) represent a significant decline in non-infected cell culture after 1 and 3 days. Data indicate no significant changes in these parameters.

3.5 Functionality of FRET-based calcium sensor

Freshly isolated ventricular myocytes were infected with the virus following 4h plating and fluorescence could already be detected within 16h. The functionality of the transferred gene was verified by monitoring $[Ca^{2+}]_i$. Figure 7 shows two typical fluorescence signal emissions measured in troponenon-expressed cells obtained at 485 nm and 535 nm excitation (upper panel). The lower panel shows the ratio of the citrine

and CFP emitted signals representing the changes of the $[Ca^{2+}]_i$ levels in the studied cells. This measurement clearly shows that virally-encoded troponenon retained its ability of indicating $[Ca^{2+}]_i$ levels in cardiomyocytes.

4. Discussion

Recent advances of transgenesis and gene targeting technologies have heralded a new era of cellular physiology to study molecular function using genetically engineered animal models and genetically encoding vector-based gene transfer systems. Practically, the mouse is the only mammalian species in which transgenic technology efficiently works. Several transgenic and gene-targeted models have been generated for the over-expression [23, 24], and genetic ablation of key proteins [25, 26] governing cardiac structure and function.

However, the mouse is not an ideal species for modelling human disease like heart failure, myocardial infarction and arrhythmia studies, because the mouse heart has distinctly different action potential waveform due to its different underlying ionic current structure [27, 28]. Transducing foreign genes to cardiac cells of living animals is a feasible technique in several animal models; however, performing electrophysiological measurements *in vivo* is not easy therefore *in vitro* electrophysiological techniques are usually used in cultured cells for this purpose. Similar experiments were performed in a recently published work using cultured human atrial myocytes [29] and myocytes isolated from rat, a species from which producing long term cell culture is much easier.

Gene transfer to cardiac myocytes has been traditionally carried out in neonatal cells. However, these cells undergo differentiation, and as a result, this model is inappropriate for certain experiments since differentiating cells have different currents than that of from adult cells. Therefore, *in vitro* transducing of isolated cardiac myocytes can be a useful alternative for investigations of cardiovascular cell physiology and diseases.

The structural changes during culturing ventricular myocytes were studied and as well [30, 31]. These changes are associated with culturing procedures associated effects, which may change a number of physiological properties of cells in culture. Therefore, some possible alterations in the Ca^{2+} handling and sarcolemmal ionic currents may have been diminished in cultured cells.

Another potential application of our viral gene transfer strategy is to introduce siRNA for silencing pore or auxiliary ionic channel subunits underlying transmembrane ionic currents. In this study we opted for canine model, since the dog unlike the mouse and rat is known to have action potential and ionic current characteristics similar to human [32]. We have chosen the transient outward current for testing the possible effects of viral infection because I_{to} is a relatively large current and present in all cells. Also it can be relatively easily measured. The I_{to} gene structure is rather complex. The I_{to} current in canine myocytes resembles human myocytes and has a large conducting pore forming unit Kv4.3 connected with several auxiliary subunits such as KChIP2, KCNE2 and DPPX [33]. In the present work, we measured the effect of the viral infection on I_{to} and we found that the virus did not affect either the density or kinetics of I_{to} current (Fig 4).

Since their introduction more than twenty years ago of Ca^{2+}-sensitive fluorescent dyes have been used to evaluate intracellular free calcium concentration ($[Ca^{2+}]_i$) [34], enabling investigators to gain unprecedented insights into the mechanisms of cell signalling. The dynamics of changing Ca^{2+} concentrations at cellular level and well-defined subcellular spaces in excitable cells, during the course of membrane depolarization can now be understood in the context of disease processes such as cardiac arrhythmias and heart failure. Although many details of excitation-contraction

coupling were described previously, novel quantitative fluorescence techniques have significantly improved our understanding of major cell regulatory pathways.

Fluorescent dyes commonly used for Ca^{2+} imaging are based on bis(2-aminophenoxy)ethane tetraacetic acid (BAPTA) structure and subsequently on bis(2-aminoethyl ether) tetraacetic acid (EGTA) backbone conjugated to a fluorescent moiety. Fura-2, indo-1 and fluo-4 are the most widely used fluorescent dyes for monitoring intracellular [Ca^{2+}]; in their acetoxymethyl ester form they can relatively easily be loaded into cells, are relatively photostable and are well suited for reliable detection of changes in Ca^{2+} concentration under physiological conditions [35]. These Ca^{2+} indicators with low molecular weight have some important advantages as great dynamic range, increased sensitivity, high fluorescent intensity and rapid response kinetics, but also have some limitations, being not targetable and subcellular localization of dye can not be controlled [36]. Recently developed genetically encoded Ca^{2+} indicators (GECIs) are defined as optical Ca^{2+} sensors produced by the expression of specific genes. These proteins contain a light-emitting fluorescent protein unit and a Ca^{2+}-responsive unit. Troponeon, a typical member of the GECI family is composed of a calcium-binding domain carrying a variant of troponin C protein and a pair of mutant green fluorescent proteins (CFP and Citrine) engineered for fluorescence resonance energy transfer (FRET) [15]. A significant difficulty in using these new Ca^{2+} sensors is their low efficiency of transfection into several cell types, cardiomyocytes included. On the other hand, the strengths of GECIs include the following: localization can be controlled by a custom signal sequence; it can be genetically fused to a protein of interest. GECIs can be maintained within cells over days to weeks and expression level/concentration of GECIs can be well controlled by incorporating a promoter [37].

At present, in spite of permanent improvements, techniques for introducing foreign genes to cultured adult cardiomyocytes suffer from substantial limitations, such as relatively low infection efficacy and/or cell surviving rate for the integration of transgenes be delivered [38, 39]. In addition, a number of studies demonstrated that vector associated cytotoxic effects directly affect a number of (electro) physiological properties of the cells [1].

In this study, we demonstrated that pseudorabies virus vectors can effectively penetrate cultured dog cardiomyocytes and that the transferred foreign gene (troponeon) could be detected already at 16 hours following infection and until at least four days post-infection. Furthermore, we showed that infected cardiomyocytes tolerated the presence of PRV vector since their electrophysiological properties were not fundamentally changed by the virus. The survival of the cells suitable for electrophysiological studies even after 4 days was high enough, proving that the virus entered the cells, did not cause any observable substantial cytotoxic effects; moreover the cells displayed unaltered electrophysiological properties. This was analyzed by 1) measuring the properties of a specific trans-membrane ionic current, the transient outward current (I_{to}), which is known to be ubiquitously present in all ventricular myocytes; 2) analyzing the intracellular Ca^{2+} transient by FRET. In these measurements we found that I_{to} was present in all cells even after 72 hours of viral infection, and neither the density nor the kinetics was different than that of observed in control cells (Fig 4). On the other hand we found that the kinetics of the intracellular Ca^{2+} transient was not significantly different between infected and non-infected cells (Fig 5, 6). Specifically, we found that infected adult dog myocytes had a lower rate of physiological degradation than that of the non-infected control cell culture in every parameter. One possible explanation for this unexpected result is that delayed apoptosis

was induced by the virus infection probably by inactivating the caspase system [40]. Recent studies have suggested that the latency-associated transcript (LAT) region of herpes simplex virus type 1 (HSV-1) is effective at blocking virus-induced apoptosis in vitro in various cell types [41, 42]. Alternatively, since anti-apoptotic effects depend on intracellular Ca^{2+} level [43], it is possible that Ca^{2+} level was decreased by binding a portion of Ca^{2+} to troponeon therefore the lower Ca^{2+} level inhibited cell death. However, the verification of this effect needs further investigation.

Conclusions

We have developed a PRV-based vector for delivery of genetically encoded activity sensors to cultured canine cardiomyocytes. This system has several advantageous features: the virus enters to cells without destroying the intact physiological properties of the cells it for a prolonged period; the virus does not change the measured physiological properties. We tested the survival rate, physiological changes on ionic current, contractile function and Ca^{2+} signalling under effect of virus mediated gene transfer in cultured adult canine cardiomyocytes. Our results show that novel herpesvirus-based vectors can transduce genes efficiently into non-dividing cardiac myocytes. Future studies are required to evaluate, whether PRV will be effective for *in vivo* infection for physiological research or gene therapeutic application.

Acknowledgements

This work was supported by grants from the Hungarian Scientific Research Fund (OTKA NI-61902, F-67879, K-68911 to A. Varró and by: T049171 to Z. Boldogkői), Human Frontiers Science Program Young Investigator grant to Z.B.; Hungarian Ministry of Health (T-353/2006, T-483/2006 and T-542/2006), the National Office for Research and Technology – Ányos Jedlik Programme TECH_08_A1_CARDIO08), European Community (EU FP6 grant LSHM-CT-2005-018833, EUGeneHeart; EU FP6 grant LSHM-CT-2006-018676, NORMACOR; EU FP7 grant ICT-2008-224381, preDiCT) and by the Hungarian Academy of Sciences, and GVOP. We thank Dr. Oliver Griesbeck (Max Planck Institute of Neurobiology, Martinsried, Germany) for providing TN-L15.

References

[1] Melo LG, Pachori AS, Kong D, Gnecchi M, Wang K, Pratt RE, et al. Gene and cell-based therapies for heart disease. FASEB J. 2004 Apr; 18(6): 648-63.

[2] Ly H, Kawase Y, Yoneyama R, Hajjar RJ. Gene therapy in the treatment of heart failure. Physiology (Bethesda). 2007 Apr; 22: 81-96.

[3] Guzman RJ, Lemarchand P, Crystal RG, Epstein SE, Finkel T. Efficient gene transfer into myocardium by direct injection of adenovirus vectors. Circ Res. 1993 Dec; 73(6): 1202-7.

[4] Donahue JK, Kikkawa K, Johns DC, Marban E, Lawrence JH. Ultrarapid, highly efficient viral gene transfer to the heart. Proc Natl Acad Sci U S A. 1997 Apr 29; 94(9): 4664-8.

[5] Schulick AH, Newman KD, Virmani R, Dichek DA. In vivo gene transfer into injured carotid arteries. Optimization and evaluation of acute toxicity. Circulation. 1995 May 1; 91(9): 2407-14.

[6] Poller W, Fechner H, Noutsias M, Tschoepe C, Schultheiss HP. Highly variable expression of virus receptors in the human cardiovascular system. Implications for cardiotropic viral infections and gene therapy. Z Kardiol. 2002 Dec; 91(12): 978-91.

[7] Nalbantoglu J, Pari G, Karpati G, Holland PC. Expression of the primary coxsackie and adenovirus receptor is downregulated during skeletal muscle maturation and limits the efficacy of adenovirus-mediated gene delivery to muscle cells. Hum Gene Ther. 1999 Apr 10; 10(6): 1009-19.

[8] Maeda Y, Ikeda U, Shimpo M, Ueno S, Ogasawara Y, Urabe M, et al. Efficient gene transfer into cardiac myocytes using adeno-associated virus (AAV) vectors. J Mol Cell Cardiol. 1998 Jul; 30(7): 1341-8.

[9] Du L, Kido M, Lee DV, Rabinowitz JE, Samulski RJ, Jamieson SW, et al. Differential myocardial gene delivery by recombinant serotype-specific adeno-associated viral vectors. Mol Ther. 2004 Sep; 10(3): 604-8.

[10] Sakoda T, Kasahara N, Hamamori Y, Kedes L. A high-titer lentiviral production system mediates efficient transduction of differentiated cells including beating cardiac myocytes. J Mol Cell Cardiol. 1999 Nov; 31(11): 2037-47.

[11] Zhao J, Pettigrew GJ, Thomas J, Vandenberg JI, Delriviere L, Bolton EM, et al. Lentiviral vectors for delivery of genes into neonatal and adult ventricular cardiac myocytes in vitro and in vivo. Basic Res Cardiol. 2002 Sep; 97(5): 348-58.

[12] Boldogkoi Z, Szabo A, Vrbova G, Nogradi A. Pseudorabies virus-based gene delivery to rat embryonic spinal cord grafts. Hum Gene Ther. 2002 Apr 10; 13(6): 719-29.

[13] Boldogkoi Z, Sik A, Denes A, Reichart A, Toldi J, Gerendai I, et al. Novel tracing paradigms--genetically engineered herpesviruses as tools for mapping functional circuits within the CNS: present status and future prospects. Prog Neurobiol. 2004 Apr; 72(6): 417-45.

[14] Boldogkoi Z, Balint K, Awatramani GB, Balya D, Busskamp V, Viney TJ, et al. Genetically timed, activity-sensor and rainbow transsynaptic viral tools. Nat Methods. 2009 6(2): 127-130.

[15] Heim N, Griesbeck O. Genetically encoded indicators of cellular calcium dynamics based on troponin C and green fluorescent protein. J Biol Chem. 2004 Apr 2; 279(14): 14280-6.

[16] Kaplan AS, Vatter AE. A comparison of herpes simplex and pseudorabies viruses. Virology. 1959 Apr; 7(4): 394-407.
[17] Boldogkoi Z, Braun A, Antal J, Fodor I. A restriction cleavage and transfection system for introducing foreign DNA sequences into the genome of a herpesvirus. Res Virol. 1998 Mar-Apr; 149(2): 87-97.
[18] Elhai J, Wolk CP. A versatile class of positive-selection vectors based on the nonviability of palindrome-containing plasmids that allows cloning into long polylinkers. Gene. 1988 Aug 15; 68(1): 119-38.
[19] Boldogkoi Z, Braun A, Fodor I. Replication and virulence of early protein 0 and long latency transcript deficient mutants of the Aujeszky's disease (pseudorabies) virus. Microbes Infect. 2000 Sep; 2(11): 1321-8.
[20] Boldogkoi Z, Erdelyi F, Fodor I. A putative latency promoter/enhancer (P(LAT2)) region of pseudorabies virus contains a virulence determinant. J Gen Virol. 2000 Feb; 81(Pt 2): 415-20.
[21] Varro A, Balati B, Iost N, Takacs J, Virag L, Lathrop DA, et al. The role of the delayed rectifier component IKs in dog ventricular muscle and Purkinje fibre repolarization. J Physiol. 2000 Feb 15; 523 Pt 1: 67-81.
[22] Birinyi P, Toth A, Jona I, Acsai K, Almassy J, Nagy N, et al. The Na+/Ca2+ exchange blocker SEA0400 fails to enhance cytosolic Ca2+ transient and contractility in canine ventricular cardiomyocytes. Cardiovasc Res. 2008 Jun 1; 78(3): 476-84.
[23] Adachi-Akahane S, Lu L, Li Z, Frank JS, Philipson KD, Morad M. Calcium signaling in transgenic mice overexpressing cardiac Na(+)-Ca2+ exchanger. J Gen Physiol. 1997 Jun; 109(6): 717-29.
[24] Chossat N, Griscelli F, Jourdon P, Logeart D, Ragot T, Heimburger M, et al. Adenoviral SERCA1a gene transfer to adult rat ventricular myocytes induces physiological changes in calcium handling. Cardiovasc Res. 2001 Feb 1; 49(2): 288-97.
[25] Pohlmann L, Kroger I, Vignier N, Schlossarek S, Kramer E, Coirault C, et al. Cardiac myosin-binding protein C is required for complete relaxation in intact myocytes. Circ Res. 2007 Oct 26; 101(9): 928-38.
[26] Rinne A, Littwitz C, Kienitz MC, Gmerek A, Bosche LI, Pott L, et al. Gene silencing in adult rat cardiac myocytes in vitro by adenovirus-mediated RNA interference. J Muscle Res Cell Motil. 2006; 27(5-7): 413-21.
[27] Xu H, Guo W, Nerbonne JM. Four kinetically distinct depolarization-activated K+ currents in adult mouse ventricular myocytes. J Gen Physiol. 1999 May; 113(5): 661-78.
[28] Himmel HM, Wettwer E, Li Q, Ravens U. Four different components contribute to outward current in rat ventricular myocytes. Am J Physiol. 1999 Jul; 277(1 Pt 2): H107-18.
[29] Liu X, Yang J, Shang F, Hong C, Guo W, Wang B, et al. Silencing GIRK4 expression in human atrial myocytes by adenovirus-delivered small hairpin RNA. Mol Biol Rep. 2008 Jul 18.
[30] Lipp P, Huser J, Pott L, Niggli E. Spatially non-uniform Ca2+ signals induced by the reduction of transverse tubules in citrate-loaded guinea-pig ventricular myocytes in culture. J Physiol. 1996 Dec 15; 497 (Pt 3): 589-97.
[31] Viero C, Kraushaar U, Ruppenthal S, Kaestner L, Lipp P. A primary culture system for sustained expression of a calcium sensor in preserved adult rat ventricular myocytes. Cell Calcium. 2008 Jan; 43(1): 59-71.
[32] Jost N, Virag L, Bitay M, Takacs J, Lengyel C, Biliczki P, et al. Restricting excessive cardiac action potential and QT prolongation: a vital role for IKs in human ventricular muscle. Circulation. 2005 Sep 6; 112(10): 1392-9.

[33] Radicke S, Cotella D, Graf EM, Banse U, Jost N, Varro A, et al. Functional modulation of the transient outward current Ito by KCNE beta-subunits and regional distribution in human non-failing and failing hearts. Cardiovasc Res. 2006 Sep 1; 71(4): 695-703.
[34] Grynkiewicz G, Poenie M, Tsien RY. A new generation of Ca2+ indicators with greatly improved fluorescence properties. J Biol Chem. 1985 Mar 25; 260(6): 3440-50.
[35] Knot HJ, Laher I, Sobie EA, Guatimosim S, Gomez-Viquez L, Hartmann H, et al. Twenty years of calcium imaging: cell physiology to dye for. Mol Interv. 2005 Apr; 5(2): 112-27.
[36] Palmer AE, Tsien RY. Measuring calcium signaling using genetically targetable fluorescent indicators. Nat Protoc. 2006; 1(3): 1057-65.
[37] McCombs JE, Palmer AE. Measuring calcium dynamics in living cells with genetically encodable calcium indicators. Methods. 2008 Nov; 46(3): 152-9.
[38] Communal C, Huq F, Lebeche D, Mestel C, Gwathmey JK, Hajjar RJ. Decreased efficiency of adenovirus-mediated gene transfer in aging cardiomyocytes. Circulation. 2003 Mar 4; 107(8): 1170-5.
[39] Li Z, Sharma RV, Duan D, Davisson RL. Adenovirus-mediated gene transfer to adult mouse cardiomyocytes is selectively influenced by culture medium. J Gene Med. 2003 Sep; 5(9): 765-72.
[40] Communal C, Sumandea M, de Tombe P, Narula J, Solaro RJ, Hajjar RJ. Functional consequences of caspase activation in cardiac myocytes. Proc Natl Acad Sci U S A. 2002 Apr 30; 99(9): 6252-6.
[41] Ahmed M, Lock M, Miller CG, Fraser NW. Regions of the herpes simplex virus type 1 latency-associated transcript that protect cells from apoptosis in vitro and protect neuronal cells in vivo. J Virol. 2002 Jan; 76(2): 717-29.
[42] Inman M, Perng GC, Henderson G, Ghiasi H, Nesburn AB, Wechsler SL, et al. Region of herpes simplex virus type 1 latency-associated transcript sufficient for wild-type spontaneous reactivation promotes cell survival in tissue culture. J Virol. 2001 Apr; 75(8): 3636-46.
[43] Chen X, Zhang X, Kubo H, Harris DM, Mills GD, Moyer J, et al. Ca2+ influx-induced sarcoplasmic reticulum Ca2+ overload causes mitochondrial-dependent apoptosis in ventricular myocytes. Circ Res. 2005 Nov 11; 97(10): 1009-17.

Figure legends

Figure 1 This panel shows a part of recombinant herpes virus genome. To adapt for applicability as virus vector we deleted the two ribonucleotide reductase (rr) and the early protein (ep0) genes from the virus genome by homologue recombination The rr1 and rr2 genes are in charge for production of raw material of viral DNA. The

recombinant virus is not able to productively infect post-mitotic cells without rr genes, while ep0 gene is responsible for virus reactivation from latency. Troponeon calcium sensor gene was inserted into the antisense promoter region in two copies.

Figure 2 Representative low- and high magnification transillumination of adult dog myocytes after isolation (day 0) and 1-3 days of culture (day 1, day 3). Panel A shows the yield of the myocytes before and one day after culturing and infection. The high-magnification transillumination (panel B) shows the morphology of adult dog myocytes after isolation (day 0) and 1-3 day of culture (day 1, day 3) and the morphological changes of living cells, versus the culturing time from non-infected (right) and the virus infected groups (left). After one day plated myocytes more than 80% displayed a rod-shaped morphology and healthy cross-striation. After 3 days (day 3) in culture, cells remained rod-shaped and partially cross-striated, and the main change was that cell ends became progressively more rounded.

Figure 3 Representative light (top) and fluorescent (bottom) microscopic images of cell culture, before and after 1 day and 3 days of virus infection. Expression of recombinant pseudorabies-viral troponeon transgenes appeared on high level in cultured adult dog ventricular myocytes. The isolation of adult dog left ventricular myocytes yielded more

than 80% living cells. After three days the troponeon expression and the physiological features of survival myocytes was appropriate for the physiological studies.

Figure 4 Panel A. Transient outward K current (I_{to}) recordings from control and from virus infected myocytes after 1 (A) and 3 days (B) of culture. Inset shows applied voltage protocol. Panel B shows the I_{to} current densities from control and from virus infected myocytes after 1 to 4 days long culture. Data represent means ± SEM, and n represents the number of experiments.

Figure 5 Original Ca^{2+} transients and cell contraction recording in cardiomyocytes cultured for 1 and 3 days. The top panel shows the intracellular Ca^{2+} concentration as Ca^{2+} transient fluorescent signal (F535nm), and bottom panel shows the changes in cell length.

Figure 6. This figure shows several parameters of intracellular free calcium transient such as amplitude of calcium transients (A), diastolic calcium levels (B), changes of calcium transient decay constant (C) and cell-shortening measurements (D) from recordings from control and from virus infected myocytes after 1 to 3 days long culture. Bars represent means ± SEM, and n represents the number of experiments.

Figure 7 Panel A. Original recordings from cells expressed troponeon at the excitation wavelength of 485 and 535 nm (top) and the characterized calcium transient (B) by ratio of the fluorescence intensity (FCFP 485 / FCITRINE 535) from one day after infection.

Figure legends

Table 1 This table shows the survival of non-infected and virally infected cells from day 0 to day 5. It can be seen that virally infected cells exhibit slightly better survival than non-infected cells, for which the reason remains to be ascertained.

Figure 1

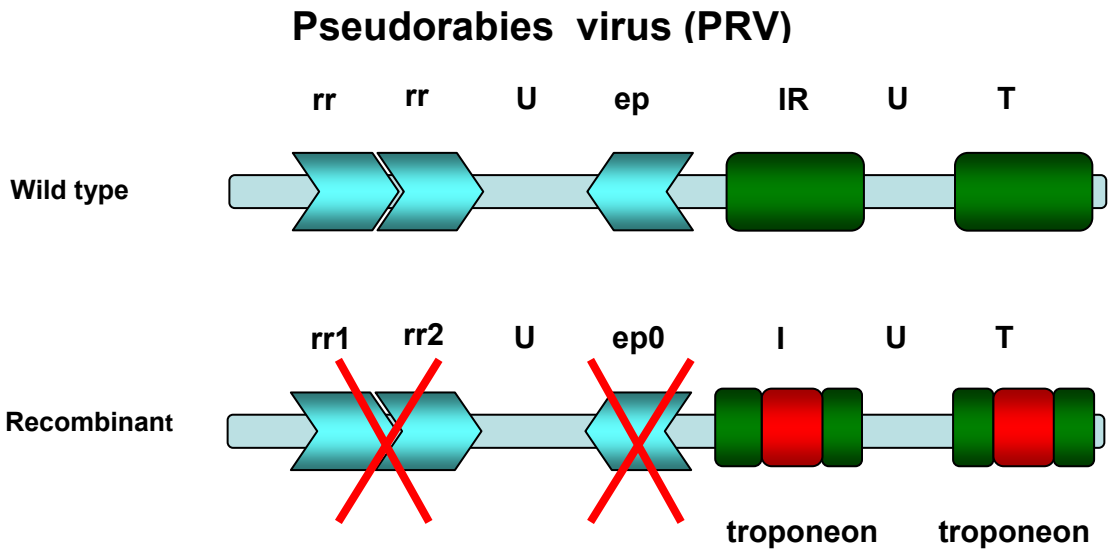

Figure 2

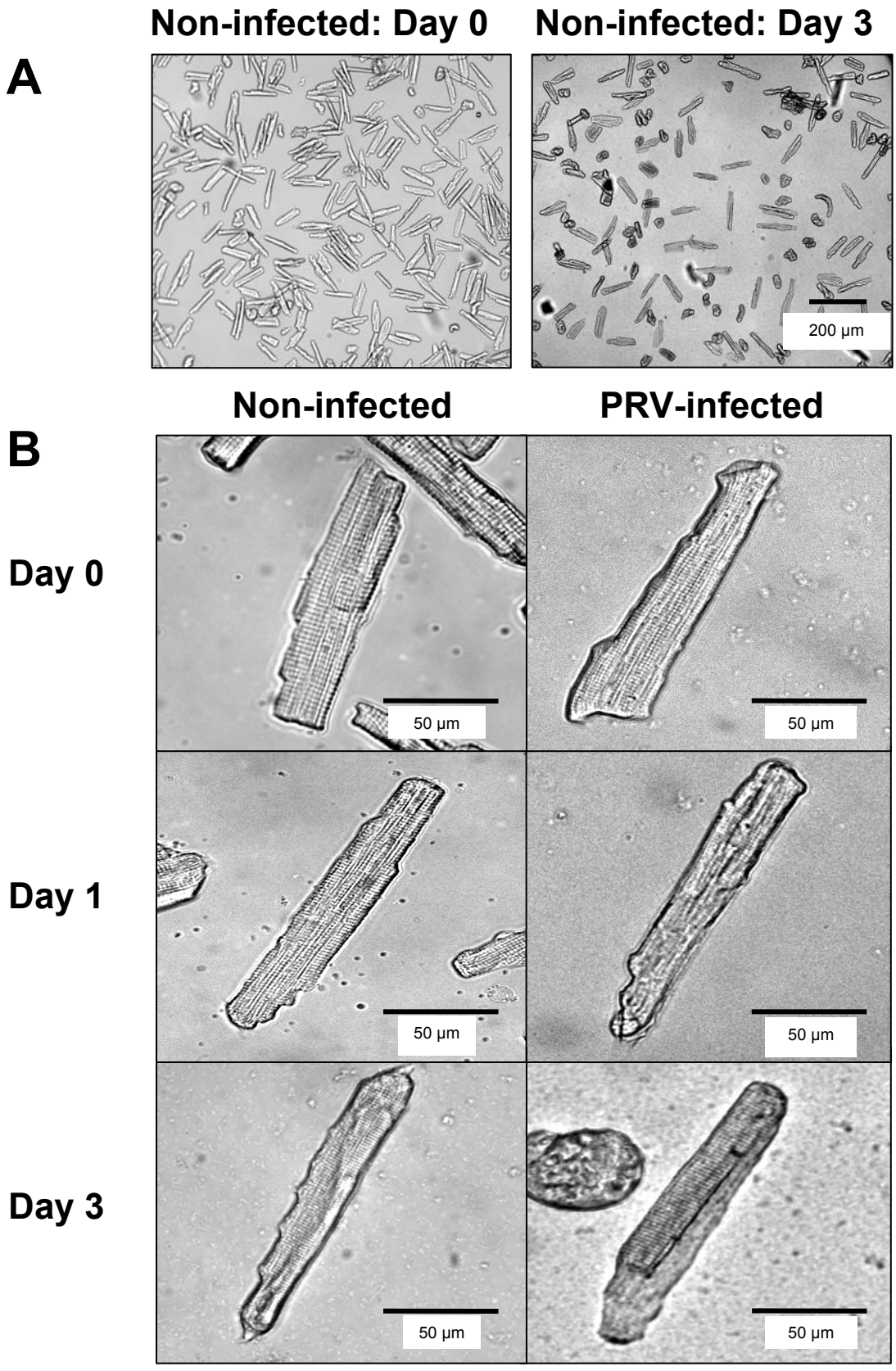
A
Non-infected: Day 0
Non-infected: Day 3
200 µm
B
Non-infected
PRV-infected
Day 0
Day 1
Day 3
50 µm
50 µm
50 µm
50 µm
50 µm
50 µm

Figure 3

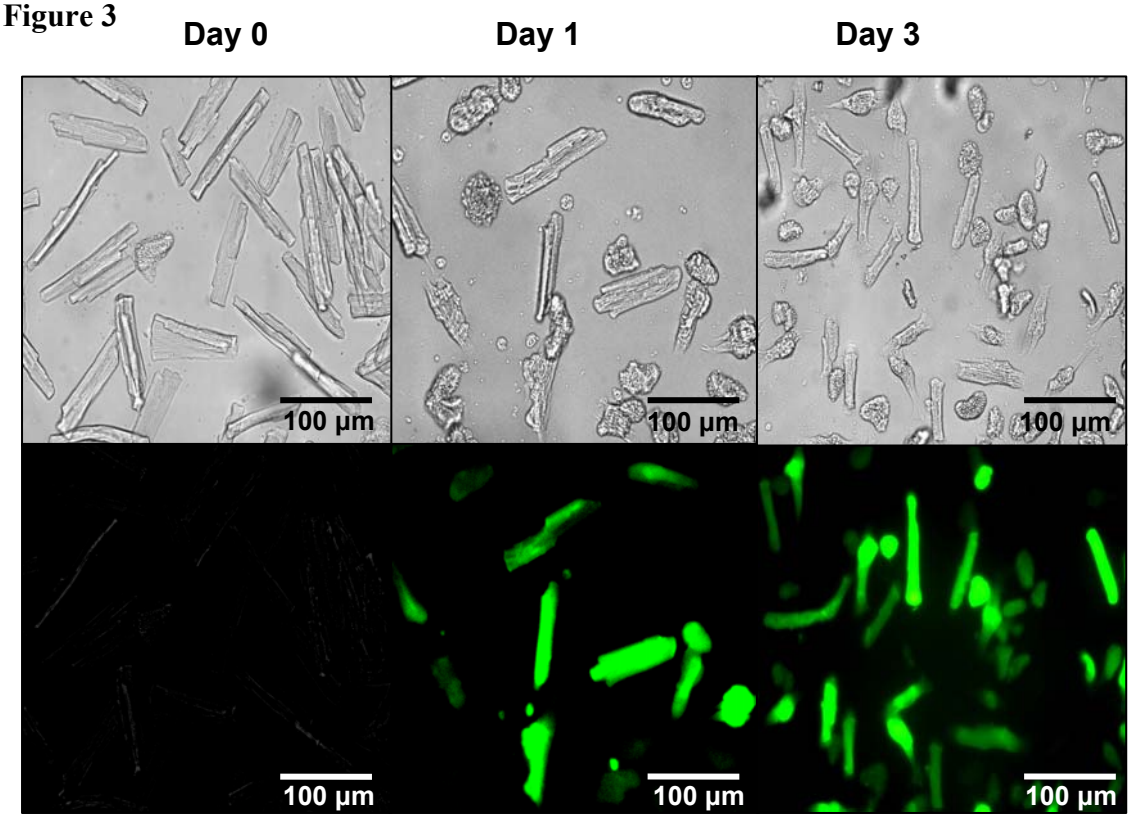

Figure 4

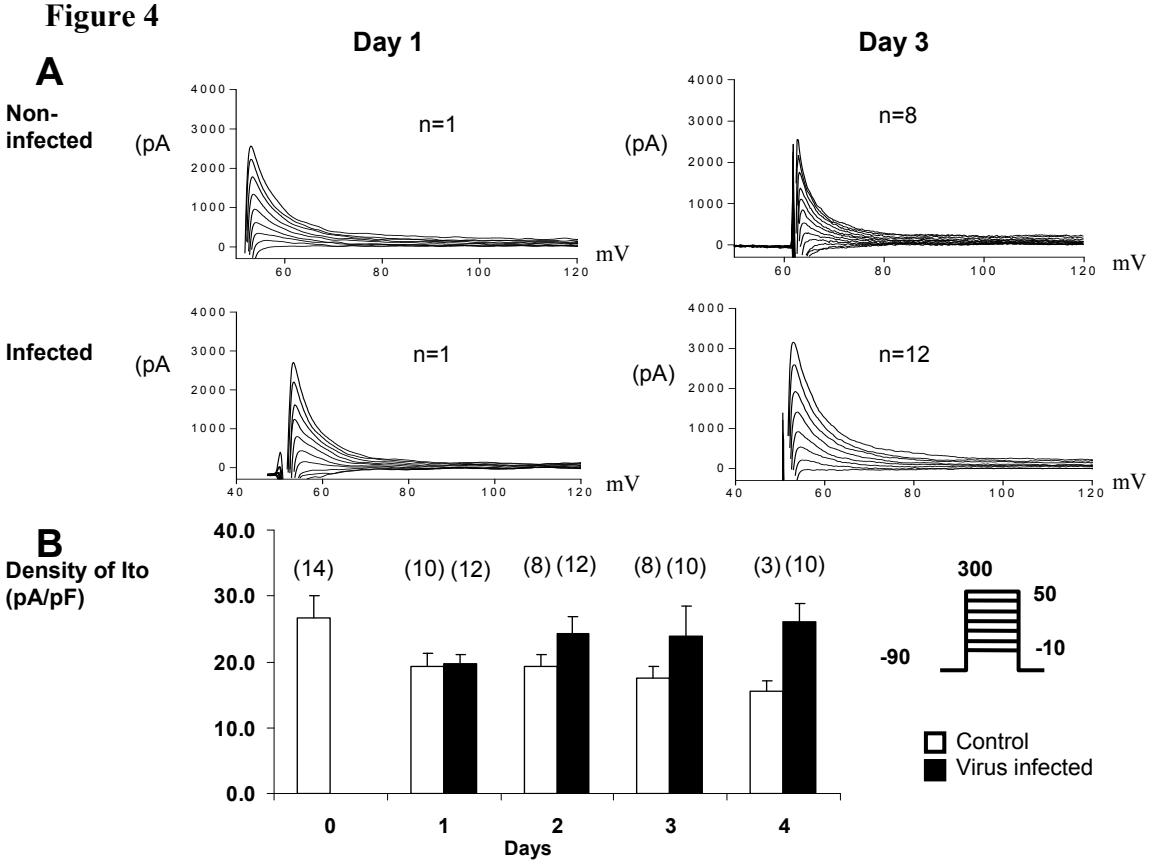
A
Day 1
Day 3
Non-infected
Infected
(pA
(pA)
n=1
n=8
n=1
n=12
mV
B
Density of Ito (pA/pF)
(14)
(10) (12)
(8) (12)
(8) (10)
(3) (10)
Days
300
50
-10
-90
Control
Virus infected

Figure 5

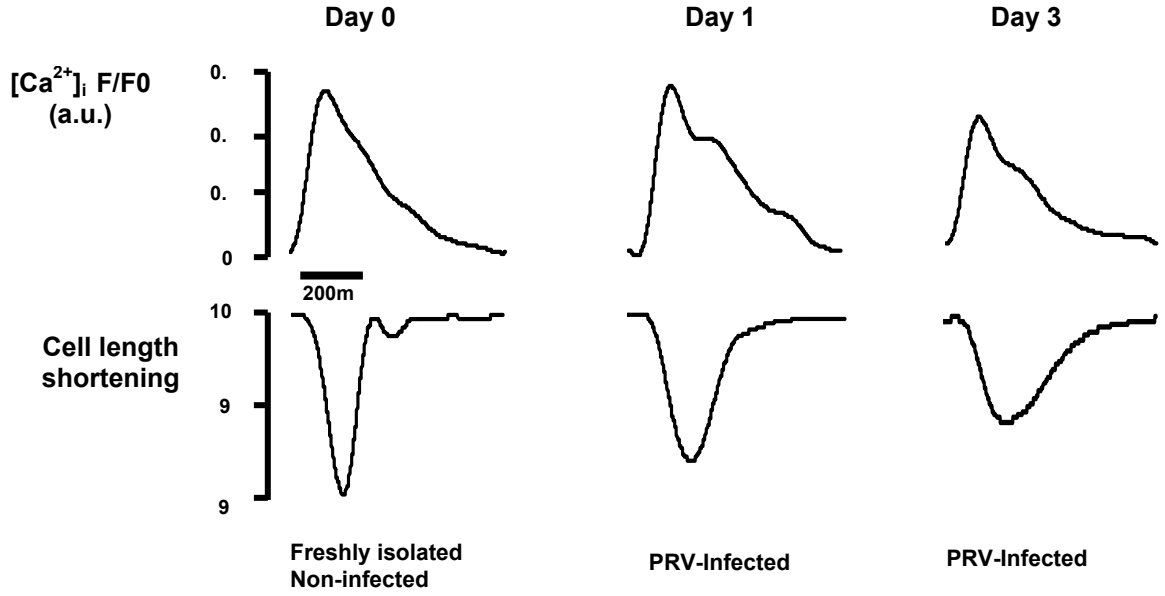
Day 0
Day 1
Day 3
[Ca2+]i F/F0
(a.u.)
0.
0.
0.
0
200m
Cell length
shortening
10
9
9
Freshly isolated
Non-infected
PRV-Infected
PRV-Infected

Figure 6

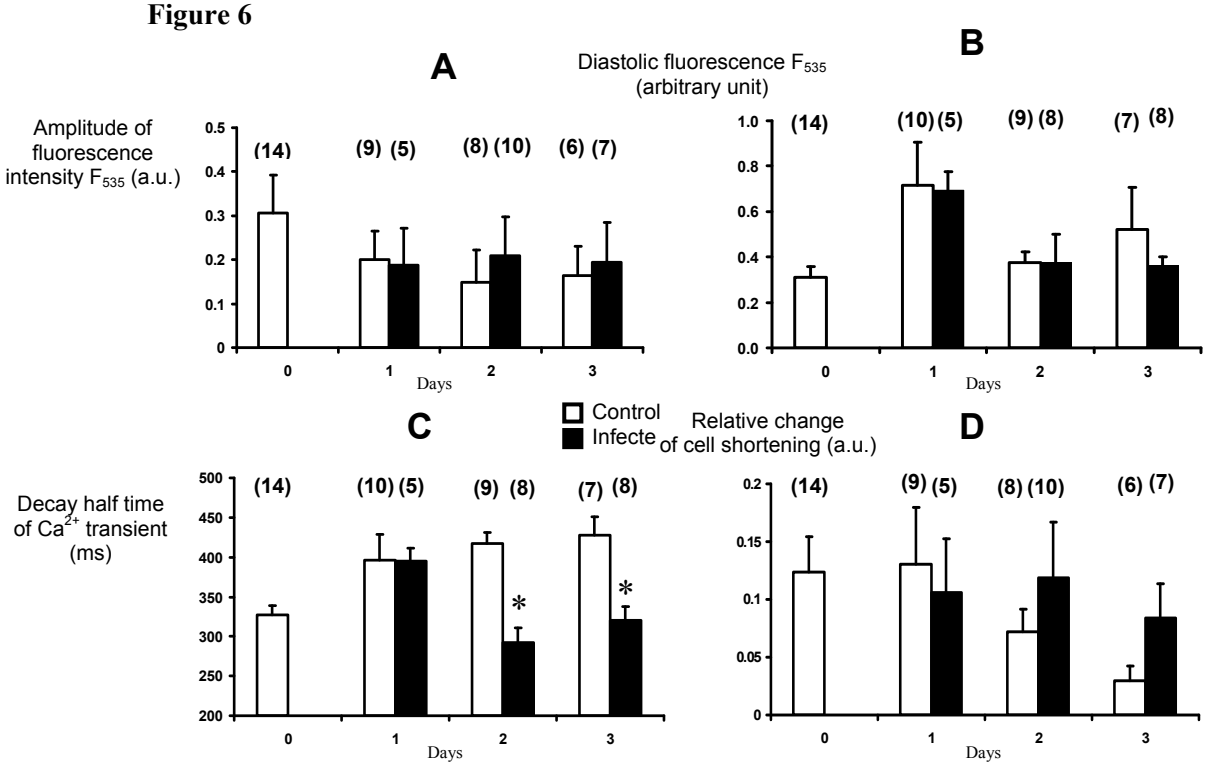

Figure 7

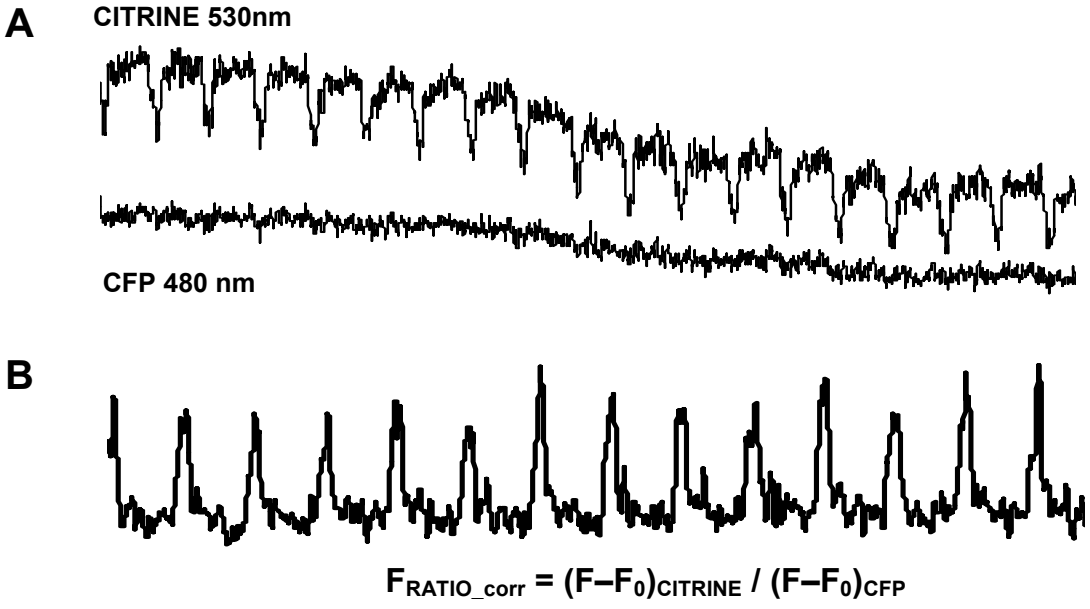

Table 1.

		Day 0	Day 1	Day 2	Day 3	Day 4	Day 5
Control	**Average (%):**	**100**	**60,0**	**44,9**	**4,3**	**2,8**	**2,2**
	Standard error:		6,0	8,4	0,5	0,3	0,3
Virus infected	**Average (%):**	**100**	**85,5**	**69,2**	**12,8**	**3,1**	**1,3**
	Standard error:		4,7	9,3	3,7	1,5	0,6